

# Comparison between numerical and experiment approach to evaluate residual stresses on dual phase steel welded by a laser YAG process

A. KOUADRI-HENNI<sup>a,b</sup>, C. SEANG<sup>a</sup>, B. MALARD<sup>c</sup>, V. KLOSEK<sup>d</sup>

a. National Institute of Applied Sciences (INSA) of Rennes, 20 Avenue des Buttes de Coësmes, 35700, Rennes, France, [afia.kouadri-henni@insa-rennes.fr](mailto:afia.kouadri-henni@insa-rennes.fr),

b. ROMAS, Laboratory of Digital Sciences of Nantes (LS2N), UMR CNRS 6004, 1 rue de la Noë, 44300, Nantes, FRANCE,

c. Université de Toulouse, CIRIMAT, INP-ENSIACET, 4 allée Emile Monso - BP44362, 31030 TOULOUSE

d. CEA de Saclay/DSM/IRAMIS/LLB

## Abstract :

*This study focused on the residual stresses (RS) generated by laser beam on a DP600 steel. During laser welding, the parts are locally heated by an intense laser beam followed by melting and solidification. The RS in the ferritic phase have been experimentally determined with neutrons techniques and numerically using Abaqus software. In this study, the elastoplastic model (VEP) includes the transformation induced volumetric strain is used to compare with the classical elastoplastic model (EP) applied to the analysis of Nd: YAG laser welding of sheet metal joining process. We simulated too the other mechanical properties to understand the influence of laser process on hardness, the tensile properties and to know if there is a relation between the RS and final mechanical behaviour. The variation of residual stresses follows the thermal cycle of laser process and so the laser parameters. The comparison between, experimental and numerical results showed the same trends considering the residual stresses in the ferrite and the studied zones. For each butt welding parameter studied, similar values were obtained. We found a relatively good correlation between experiments and numerical results with EP and VEP models, but the VM model overestimated the RS values. The FZ is in tensile with values in the order of 450 MPa. The study in the transversal direction gives the same distribution: HAZ with low values (about 30 MPa). In the longitudinal direction of the welding, the simulation results do not show differences and give us values around 450-500 MPa. In the same time, we found that the other mechanical properties present the same trends.*

**Key words:** laser process, residual stresses, dual phase steel, simulation

# 1 Introduction

In this welding process, the key parameter for microstructure optimisation and therefore mechanical properties appears to be the temperature and the heat transfer to the work pieces. These variations of mechanical properties have mainly been inputted to the initial manufacturing process of the Base Metal (BM) in the first place and then to the welding process. This study is aimed at characterizing the residual stresses (RS) distribution of a Dual Phase steel (DP600) undergoing laser beam welding. The phase transformation affects the welding process in a number of ways. Firstly, it influences the welding distortion and stresses due to their accompanied volume expansion [20] which is theoretically 1.3% of volume expansion for the austenite - ferrite transformation and 4% for austenite - martensite transformation [1]. In order to predict the welding stresses and distortions as adequate as possible, it appears to be indispensable to incorporate phase transformations in the mechanical model due to the strong spatial dependency of the phase transformations under effect of different cooling rates [2]. Studies performed by different authors [3] indicated that this volumetric expansion on cooling phase lowers the residual stresses in the fusion zone of the weld joint. Beside the physical properties of sheet metal, the welding process plays an important factor in the formation of welding pool and its evolution during cooling phase. The residual stresses along the transverse line were observed by Kong [4], the numerical and X-ray diffraction analysis had been used to study the influence of different welding processes of lap joint, laser, GTAW, hybrid laser-GTAW [5]. He found out that the maximum normal stress components are located at the HAZ and its peak value increase with the decrease in welding speed. So the implement of metallurgical effect in mechanical model is important in numerical analysis of welding residual stresses and residual distortion.

The objective of this part is to show the evolutions of the metallurgical and mechanical properties generated by the laser YAG in thin DP600 sheets. The steel DP600 was produced by Arcelor Mittal and supplied in the form of 1.5mm thick sheets. This steel grade is composed of two phases: ferrite and martensite. The sheets were coated with a fine zinc layer (0.4mm) which provides corrosion protection. This study is focused on application in the automobile industry.

## 2 Materials properties

### 2.1 Base metal properties

The standard metallographic samples of base metal and of weld cross section were prepared and examined for microstructural detail under Leica optical microscope after etching by solution Nital 4% during 10 seconds then the samples were immediately washed with water follow by ethanol, and then were blown dry in hot air. Figure 1 shows the presence of two phases in the DP600 and confirms her constituent:

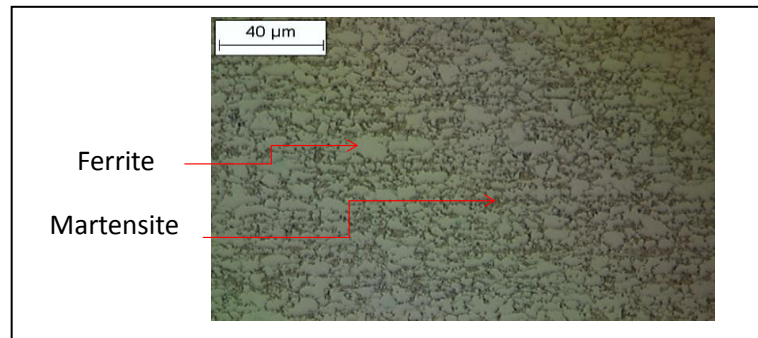


FIG1. Structure of Base Metal : 20% Martensite and 80% Ferrite

Table 1 set out the chemical composition of the base steel:

Table 1: Chemical compositions (wt. %) of DP600 steel used															
Steel	C	Mn	Mo	P	S	Si	Cr	Al	B	Ti	V	Nb	Ni	Cu	N
Wt (%)	0.07	1.4	0.2	0.0009	0.0004	0.48	0.21	0.04	-	0.01	-	-	-	-	-

The mechanical characteristics of DP600 steel are set out in table 2.

Table 2: Mechanical properties of DP600 steel used			
Steel	Yield strength (MPa)	Ultimate strength (MPa)	Elongation (%)
Wt (%)	310 ± 40	654 ± 14	23 ± 1

## 2.2 Materials properties of welded DP600 steel

### 2.2.1 Welding conditions

Experimentally, we used a laser beam, Nd:YAG, composed of the 4 kW generator with an arm robot type Fanuc R2000iB for welding operation. The diameter of the optical wire is 200 μm with a laser focus spot diameter of 560 μm and a focal length of 583.5 mm which corresponds to the focal point reference on the surface. Argon is used as a shielding gas with a flow rate of 20 CFH (Cubic Feet per Hour) on both surfaces of the blanks. To evaluate the properties of the welded joint such as the residual stresses, we welded by transparent mode the steel plates of both 1.25 mm thicknesses. A series of tests have been carried out to examine the influence of operating parameters, related to the welding environment of assemblies of thin zinc plated DP600 steel sheet, on shear strength. After the optimization, we work with following conditions: the welding was conducted at a speed of 3.4 m/min and a power of 3.5 kW in full penetration mode with thickness of 2.5 mm for the overlapping area with a lap joint gap of 0.1 mm, described by the figure 2.

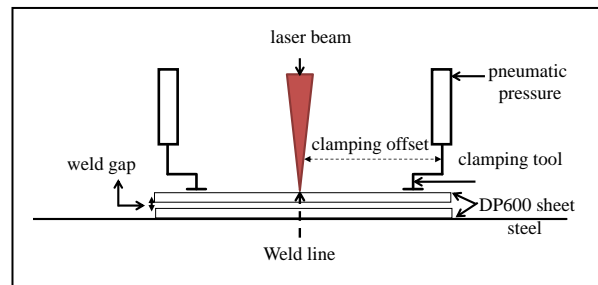


FIG 2. Principle of sketch

## 2.2.2 Microhardness

Micro-hardness survey was carried out by Mitutoyo Microhardness tester using a Vickers indenter. Hardness measurements are done along the horizontal line at the middle of the first sheet from the base metal and passing in the fusion zone and in the HAZ. The evolution is showed on the figure 3.

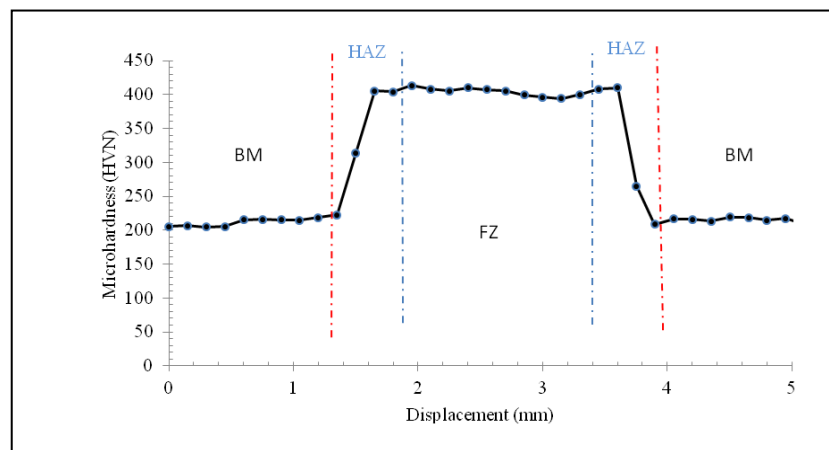


FIG.3 Hardness from the base metal passing on the heat affected zone and the welded zone close to the surface

The hardness evolution can be explained by the formation of martensite in the FZ and the HAZ. This transformation results from the rapid cooling of weld pool during laser welding process. This is the reason that cause the hardness value increases in the ZF and HAZ zone, around 400HVN as indicated in fig. 3, and depends only the volume fraction of martensite.

## 2.3 Calculation of residual stresses

We evaluated the residual stresses ( $\sigma_{11}$ ,  $\sigma_{22}$  and  $\sigma_{33}$  of the stress tensor) by neutron diffraction on the dedicated 2 axis DIANE diffractometer at Laboratory Léon Brillouin (LLB) in the ferritic phase of the plates welded in lap joint configuration by laser welding. Figure 4 presents the general principle to measure the residual deformation in the ferrite in the mid steel plate.

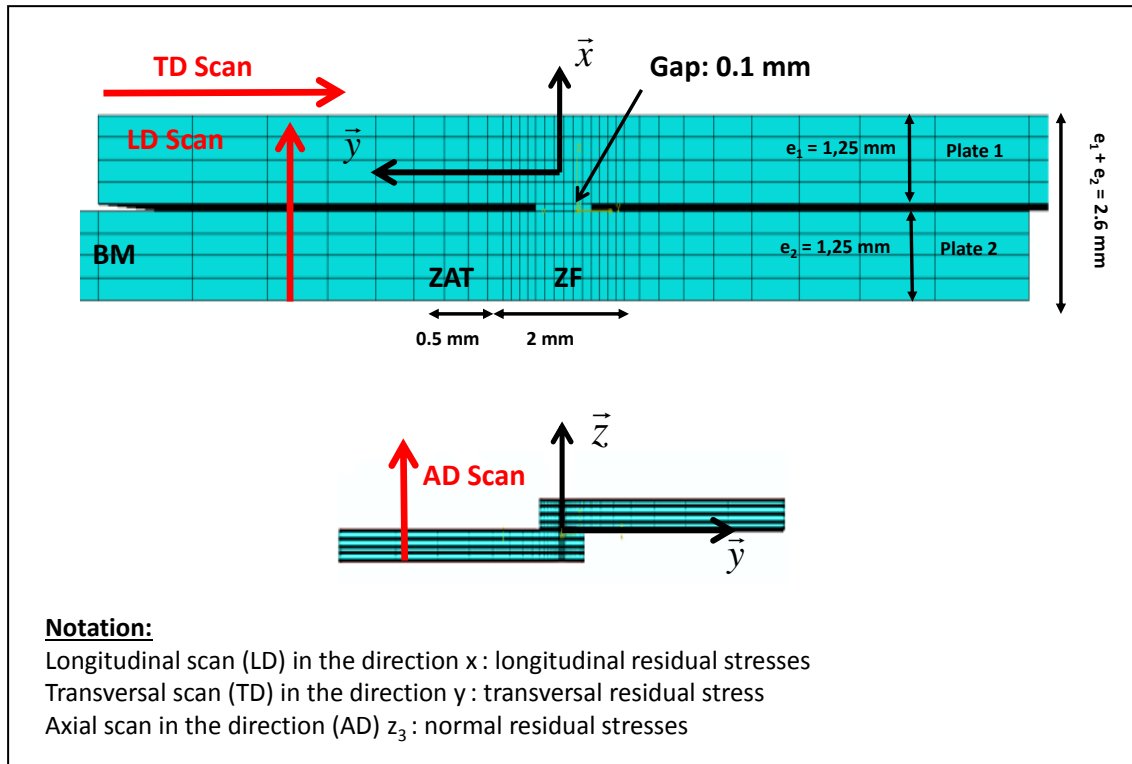


FIG 4. The different directions of the stress determination in the weld

A gauge volume of  $1 \times 1 \times 5 \text{ mm}^3$  was defined with the 5 mm aperture along the axis of the weld (to improve intensity), when possible (i.e. for transverse and longitudinal measurements only). A scan through the welded zones: BM, HAZ and FZ on the mid plate in the longitudinal and transverse directions have been performed. In a first approach, RS were calculated from the measured strains applying the Hooke's law (equation 1) in the principal directions approximation:

$$\sigma_i = \frac{E_{110}}{1 + \nu_{110}} \left[ \varepsilon_i + \frac{\nu_{110}}{1 - 2\nu_{110}} \cdot \sum_j \varepsilon_j \right] \quad (1)$$

where  $i, j$  = longitudinal, transverse and normal, and with the following values for Young modulus ( $E_{110} = 220 \text{ GPa}$ ) and Poisson's ratio (0.33).

For each measurement point because the normal stress at the surface of the plate is null, we applied the following formula, to obtain the Bragg angle corresponding to the stress free  $\theta_0$ , 110:

$$2\theta_0 = 2 \cdot \sin^{-1} \left( \frac{(1 + \nu) \cdot \sin\theta_{\text{normal}} \cdot \sin\theta_{\text{axial}} \cdot \sin\theta_{\text{transverse}}}{(1 - \nu) \cdot \sin\theta_{\text{axial}} \cdot \sin\theta_{\text{transverse}} + \nu \cdot \sin\theta_{\text{normal}} \cdot (\sin\theta_{\text{axial}} + \sin\theta_{\text{transverse}})} \right) \quad (2)$$

## 4 Numerical approach

This methodology has been already presented in an article [1] and in this paper we want to recall the principal stage. A conical heat source with Gaussian distribution [1] is used in the modeling showed on the figure 5:

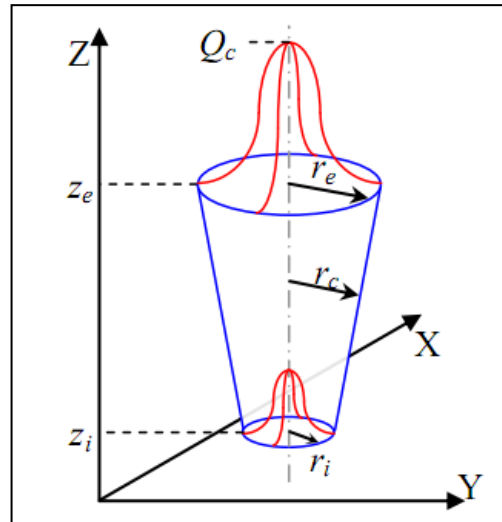


FIG.5 Conical heat source

### 4.1 Thermo-metallo-mechanical model

We built a thermo-metallo-mechanical model which takes into account the different aspects of laser welding: thermal, metallurgical and mechanical aspects. The different equations and conditions have been already described in an another article [1].

- The thermal model concerns the heat transfer from the volumetric heat source to the metal during the welding phase
- Two mathematical formulations applied during the cooling phase are:
  - The convection limits condition on the surrounding
  - The radiation limits condition on the weld pool surface :
- The metallurgical has been built from two models: the Waeckel's model [6], based on the work of Leblond [7] allows describing the anisothermal-metallurgical transformation provided by a differential equation.
- The phase transformation is described by the Koistinen and Marburger model [8].

In this part, all parameters used in this simulation were obtained from the results of thermal simulation, experiments and from the literature [9, 10]. The boundary conditions that include the convection and radiations (surrounding environment) and have been applied in the cooling step.

## 4.2 Mechanical model

• Two mechanical models have been used here, the elastoplastic model (*EP model*) and the elastoplastic with transformation induced volumetric strain model (*VEP model*). The simulation of these two models was done at the same condition and meshing parameters in order to evaluate their different outputs such as RS. The relationship of deformation is described in the following case (equation 3):

$$\varepsilon = \varepsilon^e + \varepsilon^{th} + \varepsilon^p + \varepsilon^{VEP} \quad (3)$$

where  $\varepsilon^e$  is the elastic strain,  $\varepsilon^{th}$  is the thermal strain,  $\varepsilon^p$  is the plastic strain and  $\varepsilon^{VEP}$  is the transformation induced volumetric strain. The phase transformation plays an important role in modelling the residual stresses. To count for these changes in volume, the thermal deformation is replaced by a thermo-metallurgical strain or transformation induced volumetric strain [11, 12, 13], described in the equation (4):

$$\varepsilon^{thm} = (1 - Z) \cdot (\alpha_\gamma (T - T_{\gamma ref}) - \Delta\varepsilon_{\alpha\gamma}^{20^\circ C}) + Z \cdot (\alpha_\alpha (T - T_{\alpha ref})) \quad (4)$$

Where Z is the proportion of  $\alpha$  ferritic phase,  $\varepsilon_\alpha^{th}$ ,  $\varepsilon_\gamma^{th}$  are respectively the thermal expansion of the ferritic phase  $\alpha$  and austenitic phase  $\gamma$ .  $\Delta\varepsilon_{\alpha\gamma}^{20^\circ C}$  is the different thermal strain between the two phases. The boundary condition plays an important role in the formation of residual stresses and deformation of the welded joint. Different conditions have been taking into account in this work.

## 5 Results and discussion

The comparison of residual stresses along the transverse line is the longitudinal residual stresses  $\sigma_{11}$  and the transverse residual stresses  $\sigma_{22}$ . The results in the different zones and obtained by the experiments and the simulation are presented in the table 3:

<b>Table 3: Residual stresses in different zones in different directions (Experiments)</b>			
Component	BM	HAZ	FZ
$\sigma_{11}$	300	180	320
$\sigma_{22}$	- 20	20	385
<b>Residual stresses in different zones in different directions (EP model)</b>			
Component	BM	HAZ	FZ
$\sigma_{11}$	200	180	320
$\sigma_{22}$	-20	27	344
<b>Residual stresses in different zones in different directions (VEP model)</b>			
Component	BM	HAZ	FZ
$\sigma_{11}$	180	123	310
$\sigma_{22}$	-10	27	288

Some variations are observed in longitudinal and transversal stresses. Low compressive transversal stresses are observed in the base metal close to the HAZ whereas tensile stresses are observed in the fusion zone. This is the well-known evolutions that were generally described in laser residual stresses [14]. An increase in the tensile transverse longitudinal stresses is observed in the fusion zone. These observations are due to the higher and lower temperature generated respectively in the FZ and in the HAZ, leading to a temperature gradient occurring in a narrower zone and then tensile residual stresses generated. Concerning the comparison between, experimental and numerical results showed the same trends considering the RS in the ferrite and the studied zones. The values of residual stresses show that the two models EP and VEP give almost the same value with just a few different on its intensity was found. The VEP model gives a lower values of the longitudinal residual stresses  $\sigma_{11}$ , the transverse residual stresses  $\sigma_{22}$  than those of the EP model. The difference can be considered to be negligible small.

## 5 Conclusion

This study focused on the RS generated by laser beam on a DP600 steel. During laser welding, the parts are locally heated by an intense laser beam followed by melting and solidification. In our work, the RS of a 2.5 mm thick plate are simulated and then validated with experiments using neutron diffraction technique. The major contribution of this study is the comparison between two approaches: numerical and experimental. The magnitudes of maximum RS are located in the FZ and a decreasing in the HAZ. These observations are due to the higher and lower temperatures generated respectively in the FZ and in the HAZ, leading to a temperature gradient occurring in a narrower zone hence generating higher RS. The effect of transformation induced volumetric strain had been identified using different mechanical models. The values of residual stresses such as the transverse residual stresses show clearly the different residual stresses from these models. The VEP models give a slightly lower value of longitudinal residual stresses  $\sigma_{11}$  and transversal residual stresses  $\sigma_{22}$  than that of the EP model. Anyway the different of residual stresses of these models is very low and can be considered being negligible small. One can conclude that the transformation induced volume strain has less affect on the results of the elastoplastic model for the residual stresses analysis of laser welding. This is the well-known RS evolutions that were generally described in laser welding using different models [15, 16, 17]. From simulation point of view, future perspectives are to integrate the crystallography texture and the grain orientation to better evaluate the residual stresses.

## References

- [1] A. Kouadri-Henni, C. Seang, B. Malard, V. Klosek. Residual stresses induced by laser welding process in the case of a dual-phase steel DP600: Simulation and experimental approaches. *Mater. & Des.*, 123, 89–102 (2017).
- [2] J.M. Costa, J.T.B. Pires, F. Antunes, J.P. Nobre, L.P. Borrego. Residual stresses analysis of ND-YAG laser welded joints. *Eng. Failure Anal.*, 17(1), 28-37 (2010).
- [3] J. Sun, X. Liu, Y. Tong, D. Deng. A comparative study on welding temperature fields, residual stress distributions and deformations induced by laser beam welding and CO<sub>2</sub> gas arc welding. *Mater. & Des.*, 63, 519-530, (2014).
- [4] Fanrong Kong and Radovan Kovacevic. 3d finite element modeling of the thermally induced residual stress in the hybrid
- [5] M. Z. Ul Abdein, D. Nelias, JF Jullien, D. Deloison. Prediction of laser beam welding-induced distortions and residual stresses by numerical simulation for aeronautic application. *J. of Mater. Process. Techn.*, 209(6), 2907 – 2917 (2009).
- [6] P. Dupas, F. Waeckel, A. Andrieux. Thermo-metallurgical model for steel cooling behaviour: Proposition, validation and comparison with the Sysweld's model, *J. PhysiqueIV* (6) (1996) (EDP Sciences).
- [7] J.B. Leblond and J. Devaux. A new kinetic model for anisothermal metallurgical transformations in steels including effect of austenite grain size. *Act. Metal.*, 32(1), 137-146 (1984).
- [8] D.P. Koistinen and R.E. Marburger. A general equation prescribing the extent of the austenite-martensite transformation in pure iron-carbon alloys and plain carbon steels. *Act. Metal.*, 7(1), 59 – 60 (1959)
- [9] C. Grignon, E. Petitpas, R. Perinet, J. Condoure. Thermometallurgical modeling applied to laser welding of steels. *Inter. J. of Therm. Sc.*, 40(7), 669 – 680 (2001).
- [10] J. Trzaska, A. Jagietto, L.A. Dobrzanski. The calculation of CCT diagrams for engineering steels. *World Acad. of Mater. Sc. and Manu. Eng.*, 39, 13–20, (2009).
- [11] D. Gery, H. Long, P. Maropoulos. Effects of welding speed, energy input and heat source distribution on temperature variations in butt joint welding. *J. of Mater. Proc. Tech.*, 167(2-3), 393–401 (2005).
- [12] S. Kumar, R. Awasthi, C.S. Viswanadham, K. Bhanumurthy, G.K. Dey. Thermo-metallurgical and thermo-mechanical computations for laser welded joint in 9Cr–1Mo(V,Nb) ferritic/martensitic steel. *Mater. & Des.*, 59, 211-220 (2014).

- [13] G. Mi, L. Xiong, C. Wang, X. Hu, Y. Wei. A thermal-metallurgical-mechanical model for laser welding Q235 steel. *J. of Mater. Proc. Tech.*, 238, 39-48 (2016).
- [14] P. Martinson, S. Daneshpour, M. Koçak, S. Riekehr, and P. Staron. Residual stress analysis of laser spot welding of steel sheets. *Materials & Design*, 30(9):3351 – 3359, 2009.
- [15] Y. Javadi, M. Akhlaghi, M.A Najafabadi. Using finite element and ultrasonic method to evaluate welding longitudinal residual stress through the thickness in austenitic stainless steel plates. *Mater. & Des.*, 45, 628-642 (2013).
- [16] M. Z. Ul Abdein, D. Nelias, JF Jullien and D. Deloison. Prediction of laser beam welding-induced distortions and residual stresses by numerical simulation for aeronautic application. *J. of Mater. Process. Techn.*; 209(6), 2907-2917 (2009).
- [17] P. Dupas F. Waeckel and A. Andrieux. Thermo-metallurgical model for steel cooling behaviour: Proposition, validation and comparison with the sysweld's model. *J. of physique IV(6)*, (1996) (EDP Sciences).